ACS APPLIED MATERIALS & INTERFACES

Letter

www.acsami.org

Biofunctionalized Rebar Graphene (f-RG) for Label-Free Detection of Cardiac Marker Troponin I

Satish K. Tuteja,[†,§,⊥] Priyanka Sabherwal,[‡,⊥] Akash Deep,[*,§] Richa Rastogi,[∥] Ashok K. Paul,[§] and C. Raman Suri*[,†]

[†]CSIR-Institute of Microbial Technology, Chandigarh 160036, India

[‡]Institute of Nano Science and Technology, Mohali 160062, India

[§]AcSIR-Central Scientific Instrument Organization, Chandigarh 160030, India

[∥]Centre for Nanoscience and Nanotechnology, Panjab University, Chandigarh 160014, India

Supporting Information

ABSTRACT: One-step microwave-assisted unscrolling of carbon nanotubes to form functionalized rebar graphene (f-RG) is reported. The well-characterized f-RG on an interdigitated electrode biochip in a FET configuration showed enhanced electronic properties, as demonstrated with $I-V$ characteristics. The developed device was biofunctionalized with specific anti-cTnI antibodies exhibiting a shift of threshold voltage from −2.15 V to −0.5 V and decrease in electron mobility from 3.609×10^4 to 8.877×10^3 $cm^2\ V^{-1}\ s^{-1}$. The new sensing strategy holds great promise for its applicability in diagnostics exhibiting high sensitivity (∼1 pg/mL) and specificity toward cardiac marker (cTnI).

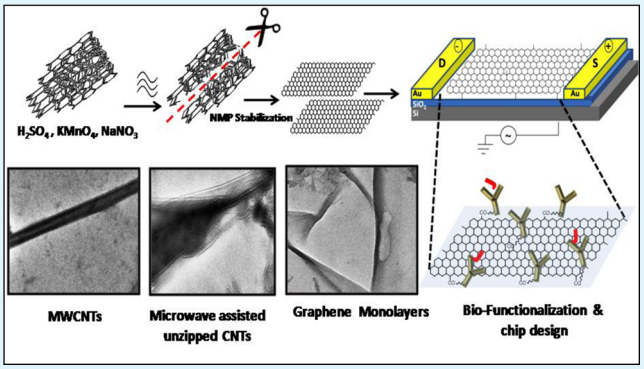

KEYWORDS: *functionalized rebar graphene, carbon nanotubes, biochip, cardiac marker, troponin I, clinical diagnostics*

Advances in molecular detection currently focus on several areas including development of new methods for quantification of a specific binding event through electrochemical or electronic measurements.[1] The development of miniaturized transducers capable of selectively determining the analyte of interest have been accomplished by using specific bioreceptors in the close proximity to CNTs, enabling them to act as one-dimensional nanochannels for electron transfer.[2−4] Typically, CNTs are prepared with aspect ratio in the range of micrometers, and usually are aggregated into macroscopically entangled ropes or heaps. However, such structural configuration of CNTs may hamper ion transport in the inner tube of CNT, especially for MWCNTs, thereby limiting their applications in the ultrasensitive detection approaches.[5] To fully realize the unique properties of MWCNTs, methods for modification at macroscopic scale have been developed by transforming them into curved graphene nanosheets.[6] Most recently, partially unzipped CNTs acting as a reinforcing bar (rebar) to form a seamless 2D conjoined hybrid through both $\pi-\pi$ stacking domains and covalent bonding has been reported.[7] The excellent electronic and spin transport properties of rebar graphene make them attractive materials in a wide range of device applications. One-step unscrolling of CNTs in transverse and longitudinal directions is still a challenging task, because of many associated problems including complex procedures and difficult manipulation. To fully realize these properties in clinical diagnostics, a reliable method for growing high quality in situ functionalized rebar graphene is very crucial. The present study describes a novel approach for synthesizing electromagnetic microwave assisted unscrolling of MWCNTs to form functionalized rebar graphene (f-RG) and demonstrated their potential applications in label-free immunosensing for the detection of human cardiac marker troponin I (cTnI). cTnI is one of the main subunits of the cardiac Troponin complex which is released into the bloodstream upon injury to cardiac muscle, particularly in myocardial infarction.[8] This potential biomarker has been recognized as "gold standard" for heart disease diagnosis due to its excellent specificity and great sensitivity for acute myocardial cell damage.[9,10] Several methods have been reported for the enhanced detection of cTnI that includes enzyme-linked immunosorbent assay, electro-chemiluminescence, fluorescence, colorimetric and surface plasmon resonance-based biosensors.[11−14] However, most of these methods are complex, which eventually increases the detection time, cost and the complexity of the sensor fabrication. Thus, the development of a rapid immunosensor for detecting cTnI in patient's serum samples is desirable due to its role in cardio specific diagnosis, risk stratification, and assessment. In our recent work, we reported lithium-ions

Received: June 4, 2014
Accepted: August 21, 2014
Published: August 21, 2014

intercalation mediated exfoliation process of graphite to form monolithic graphene sheets for the label free detection of cTnI.[15] The present work further explores the seamless 2D conjoined graphene hybrid reinforcing bar structure (f-RG) for the diagnosis of clinically important biomarker cTnI. A facile, one-step microwave-assisted modified Hummer's method was employed for the transformation of MWCNTs to f-RG. We found that microwave treatment is critical for synthesizing rebar graphene with improved surface functionality. The well-characterized f-RG functionalized with specific anti-cTnI antibodies via available functional groups (−COOH) on f-RG was immobilized on an interdigitated electrodes, and subsequently used as an ultra sensitive biochip device for the label free detection of cardiac biomarker cTnI (Figure 1).

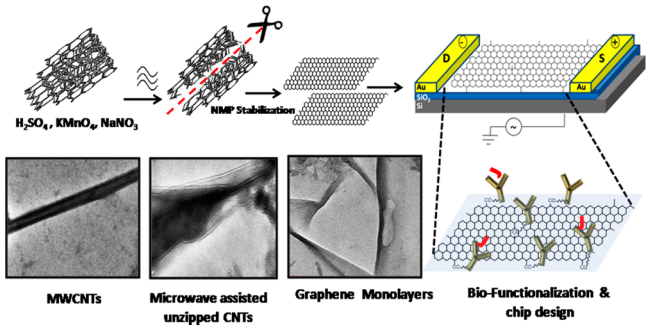

Figure 1. Microwave-induced electromagnetic transformation of MWCNTs to form functionalized rebar graphene (f-RG) to develop an ultrasensitive platform for the detection of cardiac marker troponin I (cTnI).

Functionalized rebar graphene was synthesized by facile one-step microwave assisted unscrolling of MWCNTs using electromagnetic energy mediated oxidation process (see the experimental section in the Supporting Information). MWCNTs were subjected to optimum microwave power energy (200 W) causing rapid heating because of transverse parametric resonance arising from the polarization of MWCNTs in the microwave field.[16,17] The MWCNTs were transformed to rebar graphene through change of electromagnetic energy into mechanical vibrations by surmounting the prevailing van der Waal's forces between the concentric layers of MWCNTs. This new strategy of the partial oxidative unzipping improves the selective unscrolling of MWCNTs in the longitudinal direction, presumably by the in situ protection of the vicinal diols formed in the basal plane of f-RG during microwave oxidation. The electromagnetic radiations further prevented oxidation of diols leading to the subsequent hole formation by maintaining the enhanced electronic properties of f-RG. AFM micrograph demonstrated nearly atomically smooth edges in synthesized f-RG (Figure 2a). The corresponding height profile of synthesized f-RG was observed to be around 12 nm which corresponds to ∼10 layers of rebar graphene. HR-TEM micrographs further revealed that MWCNTs are successfully unscrolled in the longitudinal direction, yielding longer fragments (∼1 μm) by showing a hybrid of flat graphene sheet and tube like structure of MWCNTs (Figure 2b). The average interlayer distance (2.5 Å) of the selected area marked as f-RG is depicted in Figure 2b (right) demonstrating crystalline order of the underlying lattice over length-scales of 2.5 nm.

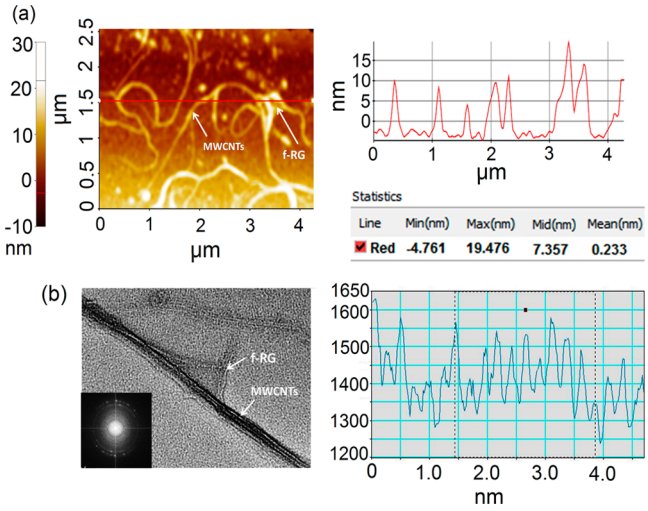

Figure 2. (a) AFM micrograph of f-RG (left) and the corresponding cross-sectional profile (right). (b) TEM micrographs of the corrugated f-RG, with fast Fourier transformed view (inset bottom left). The average interlayer distance of f-RG is shown at right.

Raman spectroscopy was performed to investigate the structural analysis of synthesized f-RG after oxidation at different microwave energies (150, 200, and 250 W). We observed characteristic D, G, and D′ Raman bands corresponding to the disorder related D band at ∼1350 cm^{-1}, the graphitic G band at ∼1600 cm^{-1}, and D′ band at ∼1620 cm^{-1} (a disorder related intravalley double-resonance Raman band).[18] The ratio of the integrated areas of D and G bands (A_D/A_G) depicting the disorder parameter taken as an indicator of the relative disorder presenting graphitic structures. With a gradual increase in microwave powers, the A_D/A_G ratios of f-RG were observed to be higher than those of MWCNTs (Figure 3a), indicating a decrease in the size of the sp^2-hybridized carbon domain during the unzipping process. A significant increase in the height of D and D′ band due to the generation of structural defects imparted by oxygenated groups in f-RG was observed which is indicative of a partial unzipping process. The oxidation of MWCNTs and the transformation of nanotubes to f-RG was measured by calculating disorder parameters at different microwave energies which were found to be 0.172, 0.733, and 1.223 corresponding to 150, 200, and 250 W respectively. The value of A_D/A_G ratio at 200 W was close to 1, indicating sufficient degree of orderness of sp^2 network in the synthesized rebar graphene. At this microwave energy, the quantification of −COOH groups on the rebar graphene was also favorable for further biofunctionalization as supported by the zeta potential studies.

FTIR spectra shown in Figure S1 in the Supporting Information depicts the peak at ∼1510 cm^{-1} which could be assigned to the aromatic C═C stretch and is attributed to the skeletal vibration of the f-RG. The peak at ∼1033 cm^{-1} is associated with C−O stretching.[19] It was further observed that the f-RG showed a very sharp characteristic peak at ∼1716 cm^{-1} originating from the stretching vibrations of C═O bonds. FTIR spectra, thus, clearly suggests the presence of −COOH groups within f-RG which could be used for biointerface development. The UV−vis spectra of MWCNTs and f-RG in solution depict peaks at 225 and 245 nm, respectively (see Figure S2 in the Supporting Information). This shift from 225 to 245 nm for f-RG indicated the increase in the degree of $\pi-\pi$

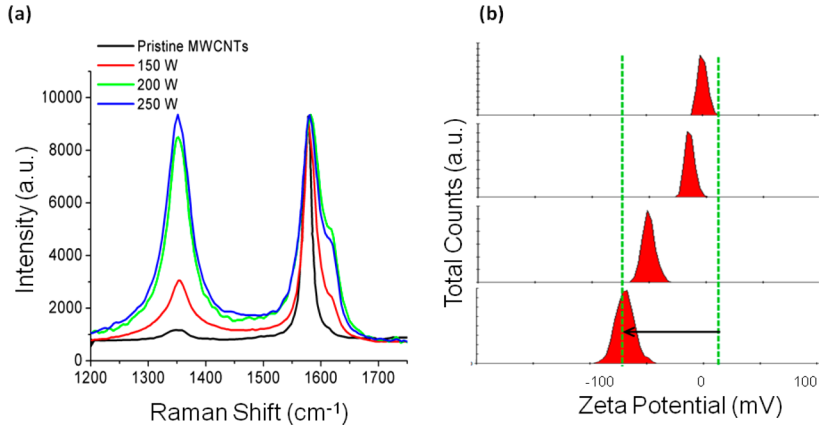

Figure 3. (a) Raman spectra of pristine MWCNTs and their subsequent transformation into f-RG at different microwave energies (150, 200, and 250 W, respectively). (b) Zeta potential studies of MWCNTs and the respective f-RG formed at different microwave energies.

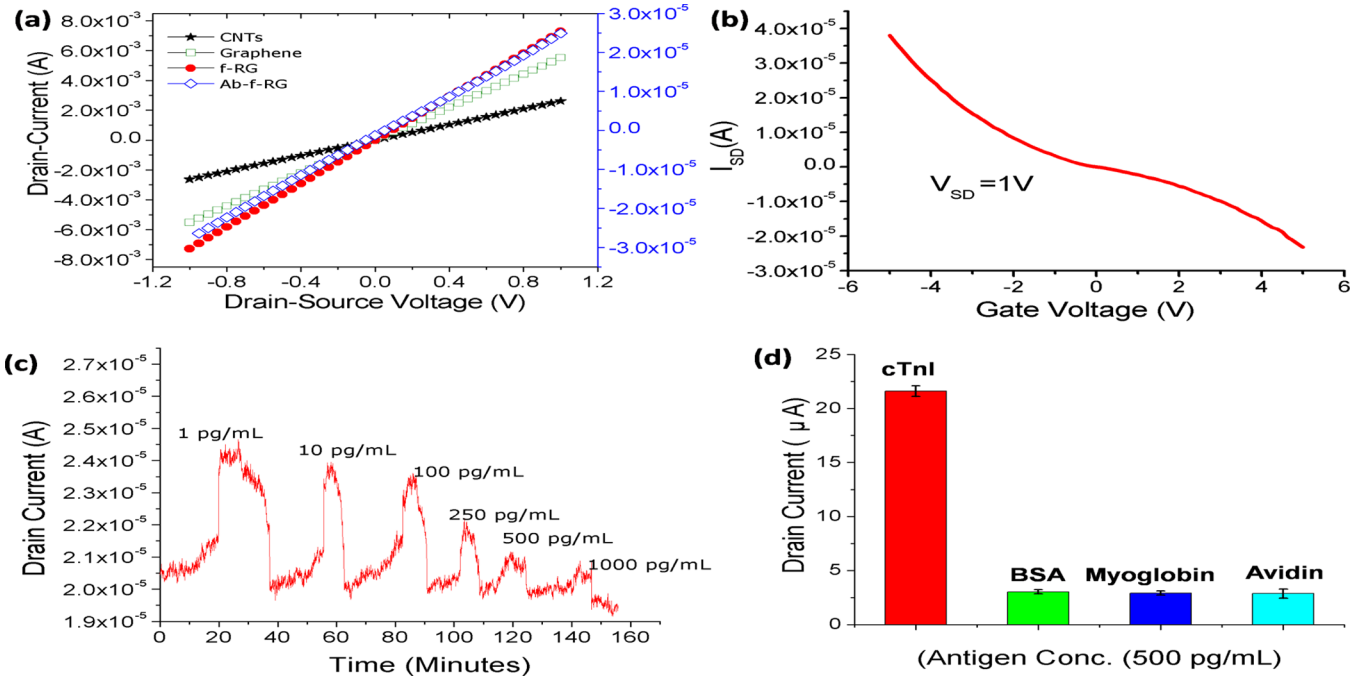

Figure 4. Current−voltage (I−V) characteristics of the device. (a) Direct current measurements of CNTs, graphene, functionalized rebar graphene (f-RG), and antibody functionalized rebar graphene (Ab-f-RG). (b) Transfer characteristics of Ab-f-RG on sensor surface. (c) Dynamic response of biofunctionalized sensor exposed to varying concentrations of cTnI (1−1000 pg/mL) (d) Bar diagrams shows the current response for cTnI and other nonspecific proteins at fixed concentration (500 pg/mL).

conjugation in f-RG as compared to pristine MWCNTs which may be attributed to in situ functionalization upon unzipping process. The zeta studies further supported the microwave energy mediated formation of f-RG by showing the zeta potential change from 0 to −60 mV (Figure 3b). The significant change in zeta toward negative side is an evident of the functionalization (−COOH) of the as synthesized rebar graphene. The thermal stability of synthesized f-RG over its precursor pristine MWCNTs was carried out by thermogravimetric analysis (TGA) and differential scanning calorimetry (DSC) observations supported an evidence for the highest stability of the synthesized f-RG on the fabricated sensor (Figure S3, Supporting Information). Also, the weight loss pattern of labile oxygen-containing functional groups and the thermokinetics studies indicated the efficient transformation of nanotubes to rebar by the incorporation of sufficient −COOH groups,[20] which are desirable for immunoassay development.

As-synthesized f-RG was drop-casted on interdigitated gold electrodes for the detection of cTnI by using label free FET configuration approach (see Figure S4 in the Supporting Information). The gold electrodes were fabricated by standard lithography procedure on a silicon chip. I−V characteristics of MWCNTs and graphene on the electrode surface revealed higher resistance in comparison to f-RG modified electrodes (Figure 4a), as graphene comprises grain boundaries of aperiodic heptagon pentagon pairs, thereby it affects electronic conductivity of graphene.[21] However, in rebar graphene nanocomposite, CNTs form networks that serve as bridges across graphene boundaries and provide greater surface area, by virtue of which the improved electronic properties are observed as compared to MWCNTs.[7] The f-RG modified interdigitated

dx.doi.org/10.1021/am503524e | ACS Appl. Mater. Interfaces 2014, 6, 14767−14771

gold electrodes functionalized with anti-cTnI antibodies were used to measure the charge transfer characteristics as shown in Figure 4b. The p-type behavior of rebar graphene was reduced significantly after antibodies immobilization on sensor surface (see Figure S5 in the Supporting Information). Further, it was observed that the Ab-f-RG device shows conduction behavior in positive gate voltage which indicates slight ambipolar behavior. Also the transconductance value (6.125 μS) and in turn mobility characteristics (8.877×10^3 cm^2 V^{-1} s^{-1}) of Ab-f-RG device decrease as compared to f-RG (3.609×10^4 cm^2 V^{-1} s^{-1}). This decrease can be attributed to the scattering of charge carries in the presence of antibody molecules at the sensor surface.[22] Additionally, a dramatic shift in threshold voltage was also observed from −2.15 V to −0.5 V. This shift toward positive gate voltages can be attributed to charge donating property of antibody molecules, which in turn are responsible for change of conduction behavior from p-type to slightly ambipolar. For assay development (Figure 4c), we incubated well-characterized Ab-f-RG electrodes with varying concentrations (1 to 1000 pg/mL) of cTnI prepared in phosphate buffer (20 mM, pH 7.5). Subsequently, $I-V$ (current−voltage) data were recorded after 20 min of incubation at room temperature. The response was linear over the range from 10 to 1000 pg/mL with a sensitivity ∼1 pg/mL of cTnI (see Figure S6 in the Supporting Information). In order to minimize non specific signals, blocking was done by using 0.01% Tween 20, prepared in PBS buffer (1X, pH 7.4). The specificity of the developed immunosensor was evaluated by measuring the response after incubating the sensor surface with cTnI specific antibodies with nonspecific proteins and other cardiac marker. The conductance remained unaffected when these non specific proteins were immobilized on the sensor surface which confirmed the specificity of the developed immunosensor toward cTnI (Figure 4d). The developed biochip demonstrates a good selectivity, high sensitivity and is capable of detecting lower cTnI concentrations in comparison to other conventional methods (see Table ST1 in the Supporting Information). The data suggest that the enhancement of assay sensitivity and specificity was achieved mainly because of the fascinating electron mobility of the functionalized rebar graphene channel with highly specific antibodies. In f-RG based FET sensor, the rebar graphene acts as the channel where resistance is monitored with respect to voltage in a concentration dependent manner of target antigen cTnI. Keeping the back electrode potential constant, we obtained a change in resistance due to the biological interactions between anti cTnI antibody and the cardiac marker cTnI. This change may be attributed to the charges induced in the f-RG channel because of the formation of antibody−antigen immune complex. It was observed that the conductance decreases gradually with increase in concentration of highly charged cTnI protein. In summary, the performance of interdigitated gold electrodes for the detection of cTnI was improved by using specific antibody functionalized rebar graphene as a new class of biofunctionalized matrix. Herein, a facile, one-step, microwave-assisted method was employed for the transformation of MWCNTs to f-RG having suitable functional groups (−COOH). The as-synthesized f-RG was employed on an interdigitated gold chip functionalized with specific anti-cTnI antibodies, which was successfully used for the development of ultra sensitive quantification of cardiac biomarker cTnI.

■ ASSOCIATED CONTENT

Ⓢ Supporting Information

Relevant experimental results and data (synthesis and characterization of f-RG, sensor design, and functionalization and specificity of developed sensor chip). This material is available free of charge via the Internet at http://pubs.acs.org.

■ AUTHOR INFORMATION

Corresponding Authors

*E-mail: raman@imtech.res.in.

*E-mail: dr.akashdeep@gmail.com.

Author Contributions

⊥S.K.T. and P.S. contributed equally.

Notes

The authors declare no competing financial interest.

■ ACKNOWLEDGMENTS

Authors acknowledge Prof. Manoj K. Rohit, Department of Cardiology, PGIMER, Chandigarh, for technical discussion and Dr. Ajay Aggarwal, CSIR-CEERI Pilani, for chip design and fabrication. S.K.T. thanks CSIR, India, for granting SRF fellowship.

■ REFERENCES

(1) Fang, Y.; Wang, E. Electrochemical Biosensors on Platforms of Graphene. *Chem. Commun.* **2013**, *49*, 9526−9539.

(2) Sharma, P.; Bhalla, V.; Tuteja, S.; Kukkar, M.; Suri, C. R. Rapid Extraction and Quantitative Detection of the Herbicide Diuron in Surface Water by a Hapten Functionalized Carbon Nanotubes based Electrochemical Analyzer. *Analyst* **2012**, *137*, 2495−2502.

(3) Qureshi, A.; Roci, I.; Gurbuz, Y.; Niazi, J. H. An Aptamer Based Competition Assay for Protein Detection using CNT Activated Gold-interdigitated Capacitor Arrays. *Biosens. Bioelectron.* **2012**, *34*, 165−170.

(4) Najafabadi, A. I.; Yamada, T.; Futaba, D. N.; Yudasaka, M.; Takagi, H.; Hatori, H.; Iijima, S.; Hata, K. High Power Supercapacitor Electrodes from Single-Walled Carbon Nanohorn/Nanotube Composite. *ACS Nano* **2011**, *5*, 811−819.

(5) Wang, H.; Wang, Y.; Hu, Z.; Wang, X. Cutting and Unzipping Multiwalled Carbon Nanotubes into Curved Graphene Nanosheets and Their Enhanced Supercapacitor Performance. *ACS Appl. Mater. Interfaces* **2012**, *4*, 6827−6834.

(6) Elías, A. L.; Méndez, A. R.; Rodríguez, D. M.; González, V. J.; González, D. R.; Ci, L.; Sandoval, E. M.; Ajayan, P. M.; Terrones, H.; Terrones, M. Longitudinal Cutting of Pure and Doped Carbon Nanotubes to Form Graphitic Nanoribbons Using Metal Clusters as Nanoscalpels. *Nano Lett.* **2010**, *10*, 366−372.

(7) Yan, Z.; Peng, Z.; Casillas, G.; Lin, J.; Xiang, C.; Zhou, H.; Yang, Y.; Ruan, G.; Raji, A. O.; Samuel, E. L. G.; Hauge, R. H.; Yacaman, M. J.; Tour, J. M. Rebar Graphene. *ACS Nano* **2014**, *8*, 5061−5068.

(8) Haaf, P.; Drexler, B.; Reichlin, T.; Twerenbold, R.; Reiter, M. High-Sensitivity Cardiac Troponin in the Distinction of Acute Myocardial Infarction From Acute Cardiac Noncoronary Artery Disease. *Circulation* **2012**, *126*, 31−40.

(9) Wang, T. J.; Wollert, K. C.; Larson, M. G.; Coglianese, E.; McCabe, E. L. Prognostic Utility of Novel Biomarkers of Cardiovascular Stress: The Framingham Heart Study. *Circulation* **2012**, *126*, 1596−1604.

(10) Apple, F. S.; Steffen, L. M.; Pearce, L. A.; Murakami, M. M.; Luepker, R. V. Increased Cardiac Troponin I as Measured by a High-Sensitivity Assay is Associated with High Odds of Cardiovascular Death: The Minnesota Heart Survey. *Clin. Chem.* **2012**, *58*, 930−935.

(11) Tate, J. R. Troponin Revisited 2008: Assay Performance. *Clin. Chem. Lab. Med.* **2008**, *46*, 1489−1500.

(12) Shen, W.; Tian, D. Y.; Cui, H.; Yang, D.; Bian, Z. P. Nanoparticle-Based Electrochemiluminescence Immunosensor with

Enhanced Sensitivity for Cardiac Troponin I Using N-(Aminobutyl)-N-(Ethylisoluminol)-Functionalized Gold Nanoparticles as Labels. *Biosens. Bioelectron.* **2011**, *27*, 18−24.
(13) Nandhikonda, P.; Heagy, M. D. An Abiotic Fluorescent Probe for Cardiac Troponin I. *J. Am. Chem. Soc.* **2011**, *133*, 14972−14974.
(14) Hasanzadeh, M.; Shadjou, N.; Soleymani, J.; Omidinia, E.; Guardia, M. D. L. Optical Immunosensing of Effective Cardiac Biomarkers on Acute Myocardial Infarction. *Trends Anal. Chem.* **2013**, *51*, 158−168.
(15) Tuteja, S. K.; Priyanka; Bhalla, V.; Deep, A.; Paul, A. K.; Suri, C. R. Graphene-Gated Biochip for the Detection of Cardiac Marker Troponin I. *Anal. Chim. Acta* **2014**, *809*, 148−54.
(16) Gemayel, M. E.; Narita, A.; Dössel, L. F.; Sundaram, R. S.; Kiersnowski, A.; Pisula, W.; Hansen, M. R.; Ferrari, A. C.; Orgiu, E.; Feng, X.; Müllen, K.; Samorì, P. Graphene Nanoribbon Blends With P3HT for Organic Electronics. *Nanoscale* **2014**, *6*, 6301−6314.
(17) Sun, C. L.; Chang, C. T.; Lee, H. H.; Zhou, J.; Wang, J.; Sham, T. K.; Pong, W. F. Microwave-Assisted Synthesis of a CoreShell MWCNT/GONR Heterostructure for the Electrochemical Detection of Ascorbic Acid, Dopamine, and Uric Acid. *ACS Nano* **2011**, *5*, 7788−7795.
(18) Sharma, P.; Bhalla, V.; Dravid, V.; Shekhawat, G.; Wu, J.; Prasad, E. S.; Suri, C. R. Enhancing Electrochemical Detection on Graphene Oxide-CNT Nanostructured Electrodes using Magneto-Nanobioprobes. *Sci. Rep.* **2013**, *877*, 1−7.
(19) Dong, J.; Yao, Z.; Yang, T.; Jiang, L.; Shen, C. Control of Superhydrophilic and Superhydrophobic Graphene Interface. *Sci. Rep.* **2013**, *1733*, 1−6.
(20) Stankovich, S.; Piner, R. D.; Nguyen, S. T.; Ruoff, R. S. Synthesis and Exfoliation of Isocyanate-Treated Graphene Oxide Nanoplatelets. *Carbon* **2006**, *44*, 3342−3347.
(21) Yan, Z.; Peng, Z.; Tour, J. M. Chemical Vapor Deposition of Graphene Single Crystals. *Acc. Chem. Res.* **2014**, *47*, 1327−1337.
(22) Wijaya, M.; Nie, T. J.; Gandhi, S.; Boro, R.; Palaniappan, A.; Hau, G. W.; Rodriguez, I.; Suri, C. R.; Mhaisalkar, S. G. Femtomolar Detection of 2,4-Dichlorophenoxyacetic acid Herbicides via Competitive Immunoassays using Microfluidic based Carbon Nanotube Liquid Gated Transistor. *Lab Chip* **2010**, *10*, 634−638.